



HAL
open science

Transient fluvial landscape and preservation of low-relief terrains in an emerging orogen: Example from Hengchun Peninsula, Taiwan

S. Giletycz, Nicolas Loget, C.P. Chang, Frédéric Mouthereau

► To cite this version:

S. Giletycz, Nicolas Loget, C.P. Chang, Frédéric Mouthereau. Transient fluvial landscape and preservation of low-relief terrains in an emerging orogen: Example from Hengchun Peninsula, Taiwan. *Geomorphology*, 2015, 231, pp.169-181. 10.1016/j.geomorph.2014.11.026 . hal-01109390

HAL Id: hal-01109390

<https://hal.science/hal-01109390>

Submitted on 26 Jan 2015

HAL is a multi-disciplinary open access archive for the deposit and dissemination of scientific research documents, whether they are published or not. The documents may come from teaching and research institutions in France or abroad, or from public or private research centers.

L'archive ouverte pluridisciplinaire **HAL**, est destinée au dépôt et à la diffusion de documents scientifiques de niveau recherche, publiés ou non, émanant des établissements d'enseignement et de recherche français ou étrangers, des laboratoires publics ou privés.

1 **Transient fluvial landscape and preservation of low-relief**
2 **terrains in an emerging orogen: example from Hengchun**
3 **Peninsula, Taiwan**

4

5 S. Giletycz¹, N. Loget^{2,3}, C-P. Chang^{1,4}, F. Mouthereau^{2,3,5,*}

6

7 Affiliation

8 ¹ Institute of Geophysics, National Central University, Chungli 320, Taiwan

9 ² Sorbonne Universités. UPMC Univ Paris 06, UMR 7193, Institut des Sciences de la
10 Terre Paris (iSTeP), 4 Place Jussieu, F-75005 Paris, France

11 ³ CNRS, UMR 7193, Institut des Sciences de la Terre Paris (iSTeP), 4 Place Jussieu, F-
12 75005 Paris, France

13 ⁴ Geological Remote Sensing Laboratory, Center for Space and Remote Sensing
14 Research, National Central University, Chungli 320, Taiwan

15 ⁵ Laboratoire International Associé ADEPT, CNRS-NSC

16 * Now at Université Toulouse III - Paul-Sabatier, Laboratoire Geoscience Environment
17 de Toulouse, UMR 5563, 14 av. Edouard Belin, F-31400 Toulouse, France

18

19 Corresponding author:

20 Slawomir Jack Giletycz

21 Department of the Earth Sciences, National Central University; address: Chongda
22 Road, 300, Chungli, Taoyuan County, Taiwan ROC; tel: (03) 4227151 ext. 57671;
23 email: geojack.slawek@gmail.com

24

25

26

27

28

29 **Abstract**

30

31 The oblique collision of Taiwan orogen led to a progressive southward uplift and
32 emergence of a submarine accretionary wedge. The Hengchun Peninsula located at
33 the southernmost tip of Taiwan island represents the most recently emerged
34 landform of an antecedent submarine surface. In this study we examine the
35 geomorphic evolution of this newly emerged and uplifted landscape. The extraction
36 of geomorphic parameters (knickpoints distribution, steepness index of rivers)
37 indicates a transient nature of the landscape but shows that a simple model of
38 regressive erosion consecutive to sudden uplift is unsatisfactory. Knickpoints
39 migration modeling shows that only the upstream Sizhong basin can be explained
40 by this single process. On the other hand, the occurrence of a relict landscape
41 (Mutan Ponds low-relief) developed at low elevations, and today uplifted in the core
42 of the peninsula, has strongly influenced the drainage evolution. Numerous
43 knickpoints are linked to capture processes around the Mutan Ponds area,
44 indicating a dynamic reorganization of the drainage system. We propose that the
45 landscape of the Hengchun Peninsula is in a transient stage and results from a
46 combination between rejuvenation and drainage rearrangement caused by the late
47 stage of emergence of the south of Taiwan.

48

49

50

51

52

53 Key words: transient landscape, orogen, Taiwan, fluvial processes, knickpoint

54 retreat

55

56 **1. Introduction**

57

58 The early stage of fluvial landscape development associated with emerging
59 mountain ranges is often difficult to capture in natural systems. First, this is because
60 the juvenile geomorphic surfaces need to be unambiguously distinguished from
61 former submarine processes that shaped the landscape. Second, they are basically
62 transient and therefore the rate at which this landscape is preserved directly
63 depends on tectonic forcing and prevailing erosional processes (Burbank, 2002).
64 Better understanding of these processes as well as the time response of landscape to
65 tectonics or climate in active areas requires an approach that aimed at quantifying
66 the early stages of geomorphic development (Willett and Brandon, 2002; Whipple,
67 2004; Crosby and Whipple, 2006; Garcia-Castellanos, 2006; Ramsey, 2006;
68 Whittaker et al., 2007; Craddock et al., 2010; Walker et al. 2011).

69 Taiwan is classically described as an active orogenic system that reached a steady-
70 state (Whipple, 2001) and where transient stages of landscape development are
71 expected to be hardly preserved. However, due to convergence obliquity that
72 induces uplift to propagate southwards (Suppe, 1981; Willett et al., 2003), the
73 southern tip of Taiwan appears to be ideally located to assess the role of outboard
74 marine inherited landscape and the geomorphic processes at play during the initial
75 stage of mountain building (Fig. 1). Previous studies in central Taiwan have shown
76 that topographic steady-state can be reached where high erosion rates 2-5 mm/yr
77 are recorded (Willett et al. 2003; Siame et al. 2011). However, in contrast to the
78 northern and more mature part of the mountain belt, the Hengchun Peninsula in the

79 south is characterized by low erosion rates as indicated by old, pre-orogenic fission-
80 track ages (Fuller et al., 2006), indicating this region did not reach an exhumational
81 steady-state. Transient stages of landscapes are mostly characterized by knickpoints
82 in their river profiles linked to a base-level drop or an increase of the tectonic uplift
83 (Whipple and Tucker, 1999; Bishop et al., 2005; Loget et al., 2006; Whittaker, 2007;
84 Attal et al., 2008; Gallen et al., 2013). Numerous works have attempted either to
85 calibrate erosional models or extract tectonic information from river profiles but in
86 most of cases they start from an inherited continental domain or antecedent
87 drainage systems (e.g., Roberts and White, 2010). Few works concern the
88 adaptation and organization of a drainage system following a large and recent
89 emerging domain (e. g., Rosenbloom and Anderson, 1994). A coupled approach of
90 river incision and organization/reorganization could be used as a marker of the
91 dynamic of emergence of continental domains.

92 In this paper, we examine the landscape evolution of the Hengchun Peninsula where
93 transient geomorphic processes, including patterns of drainage reorganization
94 (capture, knickpoints/knickzones) and relicts of low-relief high-elevation areas are
95 present. We first detailed the main geomorphic features of the peninsula
96 characterized by a N-S low-relief area pinned along the western side of the main
97 divide that are incised successively with time by the western and eastern flanks,
98 respectively. We then discuss on the origin of the main knickpoints positioned
99 around the low-relief area using a knickpoint celerity modeling approach and
100 steepness index maps. Geomorphological analyses of the large drainage basins of
101 the Hengchun Peninsula reveal that river channels recorded recent dynamics of the

102 youngest Taiwan orogen. We show that a simple rejuvenation stage cannot explain
103 the main geomorphic features. A mixed model of knickpoint propagation and
104 drainage rearrangement with captures caused by the late stage of emergence of the
105 peninsula is proposed. These erosive and landscape evolution patterns appear to be
106 compatible with an uplift originated from a deep crustal block related. The recent
107 uplift in the Hengchun Peninsula is caused by the continuing progression of the
108 collision towards the south of Taiwan.

109

110 **2. Geological background**

111 The Taiwan arc-continent collision is the result of the convergence between the
112 Chinese continental margin of the Eurasian plate and the Luzon arc belonging to the
113 oceanic Philippine Sea plate (Fig. 1). Collision started 6.5 Ma as inferred from initial
114 orogenic loading in western Taiwan (Lin et al., 2003) and onset of cooling, above the
115 underthrust continental crust, recorded at 7.1 Ma by low-temperature
116 thermochronological data (Mesalles et al., 2014). The emergence of the mountain
117 belts and coupling with surface processes become efficient after 5 Ma in northern
118 Taiwan and not before 3.5 Ma in southern Taiwan (Mesalles et al., 2014). Unreset
119 apatite fission-track ages in southernmost Central Range and Hengchun Peninsula
120 (Fuller et al., 2006; Simoes et al., 2012; Mesalles et al., 2014) argue for a slower or
121 more recent exhumation in the region with respect to the northern Taiwan. Overall,
122 these constraints are consistent with the obliquity of the convergence, implying that
123 collisional uplift and exhumation in southern Taiwan is the most recent.

124 The southward propagating model places the Hengchun Peninsula as the most lately
125 emerged region in Taiwan. As a result, the evolution of the fluvial landscape is also
126 probably the most recent, but it is yet to be determined. In particular, the patterns of
127 river captures and regressive erosion along river trunk streams have never been
128 described, thus precluding further quantification of geomorphic processes.

129 The peninsula comprises folded, non metamorphic or slightly metamorphosed,
130 Middle to Late Miocene sandstones and siltstones (Fig. 2). They correspond to
131 turbiditic sequences characterized by slope gravitational instabilities sedimentary
132 features. Lenticular conglomeratic bodies with channeling forms are locally
133 abundant and can be easily identify in the landscape due to their rough topography
134 (see Fig. 2, Shimen conglomerates). They are composed of reworked Miocene
135 sandstones, basalt, gabbros and ultramafic rocks (Pelletier and Stephan, 1986). Two
136 other sandstone members can be distinguished on the northwest and southeast tips
137 of the peninsula. Adjacent to the Miocene formation, to the west, there is the Kenting
138 ophiolitic Mélange (Kenting Formation of Fig. 2), interpreted as sheared and locally
139 faulted tectonic mélange that developed from the Late Miocene to Plio-Pleistocene.

140 The studied area is the onshore equivalent of southern accretionary prism. Its uplift
141 and exhumation appear to be driven by the accretion of a transitional crust
142 composed of the extremely-thinned continental basement of the South China Sea
143 that is tectonically stacked with Miocene post-rift deposits (McIntosh et al., 2013).

144 Well-developed Holocene marine terraces containing abundant remnants of corals
145 are found along the southern and southwestern coasts of the peninsula (Lee and
146 Liew and Lin, 1987; Chen and Liu, 1993) (Fig. 2) uplifted from few to 40 meters

147 above the sea level. Their radiocarbon dating gives ages of 10 kyr suggesting mean
148 uplift around 3.5 mm/yr during Holocene (e.g. Wang and Burnett, 1990). Coral
149 platforms corresponding to Hengchun Limestone are also observed on 200-meter
150 high cliffs of the southwestern part of the Hengchun Peninsula- Hengchun Hill
151 (Cheng and Huang, 1975; Chen and Lee, 1990)(see Fig. 2, Hengchun Limestone).
152 Their ages are estimated around Late Pleistocene (~100 ky) suggesting mean uplift
153 rates around 3-4 mm/y during Pleistocene. Few recent ages are published more
154 inland and only lacustrine deposits in Mutan Ponds low reliefs gives an age of
155 deposition between 2 and 20 ky (Yang et al., 2011). Synchronism of inland
156 lacustrine sediments and the uplifts of the Holocene marine terraces argue that the
157 uplifts of the marine terraces along the coasts could impact the deposition of the
158 Mutan Ponds within the drainage basins of the Hengchun Peninsula.

159

160 **3. Geomorphic characteristics of the Hengchun Peninsula**

161 In Taiwan, a combination of very humid and monsoonal climate coupled with active
162 tectonics causes rapid fluvial erosion forming high-relief terrains and unstable
163 slopes (Fuller et al., 2006; Ramsey et al., 2007; Giletycz et al., 2012). Heterogeneous
164 character of the rock strength or uplift results in local preservation of
165 geomorphological patterns. This particular setting gives us the opportunity to
166 examine the response of fluvial processes and landscape adjustment to short-
167 term/transient acceleration of subsurface deformations. Previous studies on Taiwan
168 geomorphology show that drainage systems ultimately control the regional
169 denudation and shape the orogen (Whipple, 2001; Wobus et al. 2006; Ramsey,

170 2006; Ramsey et al. 2007; Stolar et al. 2007). For example, Stolar et al. (2007)
171 suggested that tectonic perturbations are balanced by channel response along the
172 eastern Central Range. This contrasts with southern Taiwan where the drainage
173 system reveals ongoing dynamic adjustment.

174 Because the southward propagation of the arc-continent collision is thought to
175 occur at a rate of 55 mm/yr, Stolar et al. (2007) estimated that 1.8-2.3 Myr are
176 required to reach topographic steady-state after emergence above the sea level. Due
177 to the space-time equivalence, topographic steady-state becomes apparent at a
178 distance of 100-125 km from the southern tip of Taiwan. At this latitude individual
179 drainage basins yield rapid increase of the uplift of the southern Central Range
180 (Ramsey et al., 2007). However, Whipple (2001) argues that the timescale for the
181 Quaternary climate fluctuations and fast uplift is not enough to achieve topographic
182 steady-state, thus mountainous landscapes of Taiwan have been capable only to
183 adjust to 'mean climatic conditions'. The irregularity of the drainage system and the
184 high asymmetry of the orogen at the Hengchun Peninsula reflect its landscape to be
185 the youngest of the emerging Taiwan orogen.

186 The only geomorphological study carried out over Hengchun's Peninsula (Ramsey,
187 2006) indicates a dynamic drainage system rearrangement suggesting a short
188 duration of the geomorphic response to tectonic/climatic imprint. Ramsey (2006)
189 also suggested a lithological control for the drainage basins by the emergence of
190 Holocene coral reef limestones along the coast (Fig. 2). The uplifted limestone acted
191 as a barrier for sediments sourced from perched drainage basins, hence keeping the

192 discharge low enough to trap sediments in the upstream part of the drainage system
193 but this hypothesis hardly explains the initial shaping of low reliefs areas.

194

195 **4. Methods**

196 *4. 1. Topographic and Relief analyses*

197 Swath averaged-profiles of topography were built across the studied region to
198 report the main landscape characteristics from the Central Range in the north, down
199 to low-elevated areas of the southern Hengchun Peninsula (Fig. 3). Each profile was
200 taken perpendicular to the divide's strike where the mean, maximum and minimum
201 elevations of the DEM (SRTM 90) along an E-W 10 km window are projected into
202 cross-section planes.

203 In order to track the mean orientations of local relief in the Hengchun Peninsula, we
204 used a 3D analysis approach using a 5x5 m scale DEM (e.g. Ahnert, 1984) collected
205 by the Aerial Survey Office, Forestry Bureau- Taiwan. To carefully map the low-relief
206 areas, we adopted a circular sliding window of 5 km diameter where the mean local
207 relief (difference between the highest point and lowest point) is reported on the
208 center of this relief grid (Fig. 4).

209 Field campaigns were conducted from 2011 to 2014 to establish a direct control on
210 geomorphological features recognized from the DEM. In particular, areas of
211 potential river capture were investigated to evaluate the possible control by local
212 lithological or artefacts. Overall, field surveys allowed us to improve our
213 understanding of the incision processes in upstream regions in complement to
214 quantitative analyses.

215

216 *4.2. Steepness index and concavity index*

217 In addition to the two-dimensional topographic analysis of river profiles we
218 estimated the slope-area relationship that is characteristics of erosional processes.
219 The channel slope (S) is linked to the drainage area (A) by an inverse power law
220 such as:

221
$$S = k_s A^{-\theta} \text{ (Eq. 1)}$$

222 where (k_s) and (θ) correspond to steepness index and concavity index, respectively
223 (Hack, 1957; Flint, 1974; Snyder et al., 2000; Lague and Davy, 2003). If we assume
224 that fluvial erosion follows a detachment-limited erosional pattern, the erosion (E)
225 is governed with a stream power law such as:

226
$$E = KA^m S^n \text{ (Eq. 2)}$$

227 where K represents the erodibility of rocks, A the upstream drainage area and S the
228 local slope (Howard, 1994; Whipple and Tucker, 1999).

229 In the specific case of steady state where E equal uplift rate (U), equation 2 becomes:

230
$$S = (U/K)^{1/n} A^{-m/n} \text{ (Eq. 3)}$$

231 Where $(U/K)^{1/n}$ and $-m/n$ represent k_s and θ , respectively. In a log-log plot, θ ,
232 which is sensitive to the basin hydrology, corresponds to the slope of the regression
233 line whereas k_s is the intercept. Both k_s and θ , are known to be highly sensitive to
234 tectonic uplift (e.g., Snyder et al., 2000). The concavity θ typically varies in the small
235 range of 0.4 to 0.6. This enables us to adopt a reference concavity index (θ_{ref})
236 where different stream profiles can be directly compared by a normalized steepness
237 index (k_{sn}) (Wobus et al., 2006; Kirby and Whipple, 2012). We keep in mind that

238 these parameters are often deduced from an equilibrium stage of river profiles.
239 However for transient cases the response time of rivers may be longer than the
240 tectonic forcing as indicated by the presence of knickpoints in river profiles. In that
241 case, one may consider that knickpoint separates an upstream section in a paleo-
242 equilibrium stage from a downstream oversteepened part in a final equilibrium
243 stage (Whipple and Tucker, 1999).

244 Here, we have adopted the automated method for extraction of steepness and
245 concavity indexes on stream profiles developed by Whipple et al. (2007) on a
246 ArcGIS-Matlab environment that can be freely downloaded at *geomorphtools.org*.

247

248 *4.3. Modeling knickpoint retreat*

249 An important point concerning the morphological evolution of Hengchun Peninsula
250 is to evaluate if this landscape is a result of a uniform or more distributed uplift. A
251 uniform uplift would induce a wave of regressive erosion in a radial pattern in the
252 watersheds (Crosby and Whipple, 2006; Berlin and Anderson, 2007). By contrast, a
253 distributed uplift would induce a mixing of wave of erosion, shifting and capture of
254 rivers (e.g., Jackson et al., 1996).

255 To investigate the hypothesis of a wave knickpoint migration, we tested a
256 knickpoint celerity model. The model predicts knickpoints position at each time step
257 (Crosby and Whipple, 2006; Berlin and Anderson, 2007; Loget and Van Den
258 Driessche, 2009; Gallen et al. 2013) such as:

259
$$V = dx/dt = CA^P \text{ (Eq. 4)}$$

260 where V is upstream knickpoint migration rate, C is a constant dimensional
261 coefficient representing erodibility and efficiency of the knickpoint retreat, A is an
262 upstream area and p is a non-dimensional constant for the power law dependence
263 on a drainage area. We have considered a uniform erodibility at the scale of the
264 basin as suggested by the uniform lithology of the Mutan turbidites.

265 We hypothesized an initial upstream area or a starting point for the knickpoint
266 migration as the converging point of main knickpoints in the basin coupled to the
267 presence of knickpoints in all upstream sub-watersheds. In the absence of data for
268 incision or knickpoint migration rates, we tested two end-member classes of
269 parameters for the modeling that fit with response time around 10^4 to 10^5 years for
270 knickpoint migration. We used the model parameters of Crosby and Whipple,
271 (2006) (hereafter abbreviated CW) with $V=7.9 \cdot 10^{-7}A^{1.1125}$ (that favors large
272 upstream area with a low efficiency for knickpoint retreat) and the model of Loget
273 and Van Den Driessche (2009) (hereafter abbreviated LVDD) where $V = 10^{-4} A^{0.5}$
274 (that favors small upstream area with a high efficiency for knickpoint retreat). Both
275 models were stopped when the modeled knickpoint reach the farthest knickpoints
276 (KP5).

277

278 *4.4. Asymmetry Factor (AF) observations*

279 To highlight the areas with potential captures, we have adopted the non-
280 dimensional Asymmetry Factor (AF) (Hare and Gardner, 1985):

281
$$AF = 100(A_r/A_t) \text{ (Eq 5)}$$

282 where, A_r represents the drainage area to the right of the main trunk stream looking
283 downstream and A_t is the total drainage area. A symmetric catchment with a mean
284 value of $AF = 50$ indicates equal development of the drainage basin both on the right
285 and left side of the basin. Decrease or increase of the AF value indicates the
286 development of asymmetry on either side of the drainage area. Such asymmetry can
287 potentially emphasize an area where one drainage basin through a capture adopted
288 new tributaries. In our AF analyses we targeted small drainage basins along the
289 main divide and coasts, where the AF is more sensitive to local variances.

290

291 **5. Results**

292 *5.1 Topographic and relief analyses*

293 The Central Range of Taiwan evolves from a well-organized transverse drainage
294 system that progressively turns southwards into asymmetrical and disordered
295 drainage system stretched over the whole Hengchun Peninsula (Fig. 3). Across the
296 Central Range, the highest elevation on the swath profile (mean, maximum or
297 minimum altitudes) is located near the divide (Fig. 3a). This contrasts with the
298 Hengchun Peninsula where the highest elevation and main divide split in two
299 different eastern and western subdomains and associated divides (Fig. 3b).

300 For instance, the highest domain of the peninsula ($\sim 1000\text{m}$) is observed in the
301 Lilong Range that sets close to the western coast. Conversely, the Mutan Ponds in
302 the eastern part of the peninsula is lower ($\sim 400\text{m}$) but are located along the main
303 divide (Fig. 3b).

304 Relief map (Fig. 4) shows that the maximum local relief (between 400 m and 800 m)
305 is located in the northwest part of the Hengchun Peninsula, in the Lilong Range. The
306 southern and eastern parts of the peninsula are characterized by an alternation of
307 moderate (between 250 m and 400m) and low reliefs (lower than 250m). Figure 4
308 further reveals that the both low and high relief domains are oriented N-S.

309 The main drainage basins are Fengkang, Sizhong and Gutou (Fig. 5). They drain over
310 60% of the peninsula's surface (of the area of 3×10^2 km²), while over 20 basins
311 distributed along the coasts have drainage areas in the 2 to 5 km² range with only
312 three basins of ~ 1 km² and two of ~ 20 km². The significant feature is that
313 headwaters of the two main basins (Fengkang and Sizhong) are positioned in the
314 low-relief area of the Mutan Ponds, while their outlets set at the high-relief region in
315 vicinity of the Lilong Range.

316 They drain northern and central Hengchun Peninsula and therefore are the most
317 suitable targets to examine the fluvial network response of the landscape to the base
318 level change. Gutou drainage basin at the southern part of the peninsula flows into
319 the Pacific Ocean to the east. Its whole basin is situated in the low-relief zone and
320 together with Mutan Ponds in the north form the youngest landscape of the
321 emerging wedge (Fig. 4). Headwaters of the Fengkang, Sizhong and Gutou basins
322 begin at comparable elevations of 350-400 meters, but only Sizhong and Fengkang
323 expose apparent shrinkage of the relict landscape.

324 Fengkang basin channels expose knickpoints in the upstream area. This contrasts
325 with the Sizhong basin that is characterized by a more extensive distribution of the
326 knickpoints, probably reflecting a more dynamic response to the relative base level

327 fall. In the Gutou basin, knickpoints are apparent only in the vicinity of the drainage
328 divide (Fig. 5). East of the main divide, a number of knickpoints reveal advancing
329 fluvial processes, however their irregular vertical distribution suggest different
330 origin. Some of knickpoints located close to the main divide are related to capture
331 events of the Sizhong basin at the Mutan Ponds area.

332

333 *5.2. Long river profiles, steepness and concavity indices*

334 River profiles are commonly used to infer the uplift pattern in active tectonic area
335 (Snyder et al., 2000; Kirby and Whipple, 2001; Kirby and Whipple, 2012). We
336 extracted the main profiles of Fengkang, Sizhong and Gutou (trunk and tributaries)
337 (Fig. 6). One particular feature of these basins is that headwaters of main trunks are
338 located at low-elevation close to the Mutan ponds and are thus at lower altitudes
339 than their tributaries. None of three basins presents full graded or concave up
340 profiles arguing for a transient stage. They present numerous knickpoints and
341 knickzones that are located in the upstream part of the trunks and in the tributaries
342 that join them at a maximum distance of 10-15 km from the headwater. Knickpoints
343 are located at an altitude of about 300m in the Fengkang basin, between 200 and
344 500 m for Sizhong basin, and between 200 and 400 m for Gutou basin.

345 The slope-area relationship for Fengkang, Sizhong and Gutou main trunks show the
346 same pattern with some remarkable breaks in regression lines corresponding to the
347 position of knickpoints (Fig. 6). θ values for Fengkang river are 0.42 and 0.43
348 upstream and downstream of the break, respectively. We choose a value for θ_{ref} of
349 0.45 consistent with previous works on Taiwan (Wobus et al., 2006). This θ_{ref} value

350 corresponds to k_{sn} values of 7.19 and 33.4 upstream and downstream of the break,
351 respectively. This kind of pattern with a break in the slope-area relationship and a
352 sudden rise of k_{sn} values upstream may be interpreted as a transient profile due to
353 an increase of uplift rate (e.g., Whipple et al., 2013). We obtained similar values for
354 Sizhong's k_{sn} (9.52 to 30) but the increase is lower toward the south for Gutou basin
355 (11.3 to 16.4). We also calculated k_{sn} values at the scale of the Hengchun Peninsula
356 with the auto-ksn tool developed by Whipple et al. (2007) that allows to do
357 regression over a specified moving window (here 0.5 km) (Fig. 7). Results obtained
358 confirm the pattern observed with relief maps. Highest values of k_{sn} (60-200) are
359 located in northwest part whereas lowest values (0-15) are located in the southern
360 part and in the Mutan Ponds. With this analysis we confirm that k_{sn} values are lower
361 in the upstream part than downstream for Fengkang, Sizhong and Gutou basins.
362 This trend is not observed on rivers that flow toward the east. This reflects the fact
363 that inherited low-relief domains also characterized low k_{sn} values are confined on
364 the western side of the main divide and are incised with rivers flowing toward the
365 west.

366

367 *5.3. Modeling knickpoint retreat: Is there a wave of regressive erosion in the Hengchun*
368 *Peninsula?*

369 The only basin where k_{sn} in the main trunk is higher or in the same order than
370 tributaries is the Sizhong basin and could correspond to a local wave of regressive
371 erosion.

372 If one examines the map distribution of knickpoints on the Hengchun Peninsula,
373 they do not appear to follow a full radial pattern in the different watershed of the
374 peninsula except for the Sizhong basin (Fig. 5). We further notice that k_{sn} in main
375 trunks are not statistically higher than their tributaries (Fig. 7) as commonly
376 expected for a wave of knickpoint migration (Wobus et al, 2006). Results of
377 knickpoint migration modelling reveal that none of two end-member models can fit
378 both west and east sub-catchments of Shizong (Fig. 8). In the west sub-catchment,
379 the celerity model derived from the parameters used in CW model fits better the
380 position of the five current knickpoints than those derived from LVDD model. The
381 position of three knickpoints is well reproduced and the two others do not exceed 1
382 km of misfit assuming CW model for a time duration of 17 Ky. With the LVDD model
383 only one knickpoint is reproduced and four with misfit higher than 1 km for a time
384 duration of 36 ky. In the east sub-catchment, the LVDD model well reproduced the
385 position of one knickpoint and the other one with error of more than 1 km. In
386 contrast, the CW model reproduces both knickpoints within an error of more than 1
387 km and less than 1 km, respectively.

388 Two conclusions arise from the quantitative modeling of knickpoint retreat. First, if
389 our starting point of knickpoint migration is valid, then the response time according
390 to 10^4 - 10^5 celerity parameters can be estimated to about 17 Ky (according to the
391 best fit model) in the west sub-catchment of Sizhong. In the Hengchun Peninsula, a
392 wave of knickpoints migration can be observed but is limited to a local scale (here
393 ~ 20 km²) that excludes a uniform uplift of the whole peninsula. Second, knickpoints
394 migration both in the eastern and western sub-catchments cannot be reproduced

395 with a simple celerity modeling. By testing two end-member models that are
396 assumed to reproduce the whole range of knickpoint regressive erosion processes,
397 we rule out an incomplete parametric study. We rather suspect changes in the
398 upstream drainage area that can be explained by a process of capture of one sub-
399 catchment by another one. This piracy process could explain why the altitude of the
400 graded part of each trunk profile, for west and east sub-catchments, is different.

401

402 *5.2. River capture*

403 A significant part of knickpoints cannot be explained by a wave of regressive erosion
404 moving upstream and incising an uplifting inherited landscape. The observation of
405 capture points instead is remarkable in the Hengchun Peninsula. This argues for
406 drainage reorganization caused by piracy or capture effects, especially in the
407 Sizhong basin where this mechanism is probably the most significant. For example,
408 a number capture points can be observed along the main divide suggesting its
409 westward movement. Fieldwork investigations carried out along the main drainage
410 divide confirm very active regressive erosion upstream of the eastern drainage
411 basins (Fig. 9).

412 Figure 10 shows a good example where part of the Sizhong basin was captured by
413 eastward draining tributary of the Xuhai channel. The knickpoint observed along
414 the western tributary is very likely a capture point as indicated by the abrupt
415 change of flows above the knickpoints and the large inflexion of the divide (Fig. 10b,
416 red arrow).

417 The upstream reaches of Xuhai basin display an asymmetrical pattern (Fig. 10c).
418 Using the shape of the main drainage divide, flow direction of the tributaries
419 together with assumption that knickpoints are actually capture points, we obtained
420 a possible drainage arrangement before the capture with a symmetrical basin model
421 (Fig. 10d).

422 The regressive erosion that led to river capture is not only observed at the main
423 drainage divide. For instance, the 'pre-capture' geometry is seen in the vicinity of
424 the downstream of the Sizhong River (Fig. 11). Zhushe tributary of the Baoli River
425 flows nearly 100 meters above the meander of the Sizhong main channel. An outside
426 band of the Sizhong meander undercuts a hill slope removing western tributaries of
427 the Baoli channel. This reflects that continuous regressive erosion is currently
428 triggering a capture by merging the upper part of the Baoli basin with the Sizhong
429 basin. This will result in the migration of the drainage divide toward the east. A very
430 low Asymmetry Factor ($AF = 20$) of the central and upper part of the Baoli channel
431 confirms the role of capture dynamics.

432

433 **6. Discussion**

434 The geomorphological analysis performed on the Hengchun Peninsula argues for a
435 transient stage of the landscape evolution of the southern Taiwan (Ramsey et al.,
436 2007; Stolar et al., 2007). The presence of preserved low reliefs may be classically
437 attributed to a change of uplift not yet counterbalanced by fluvial erosion (e.g.,
438 Davis, 1989). The normalized steepness indexes of rivers (k_{sn}) are also strongly
439 correlated to relief maps (Fig. 4 and 7) with an increase of k_{sn} downstream of

440 knickpoints in all main trunks (Fig. 6). In steady-state conditions, high and low
441 values of k_{sn} represent high uplift zones and low uplift zones, respectively (Snyder et
442 al., 2000). k_{sn} values show a sudden increase in slope-area relationships along river
443 profiles that reflect an increase of the uplift rate in transient conditions (e.g.,
444 Whipple et al., 2013). This is well documented for Fengkang, Sizhong and Gutou
445 rivers (Fig. 6). Both geomorphic markers- low reliefs and k_{sn} distribution maps
446 reflect a transient landscape evolution consecutive to an increase of the uplift rate.
447 However, the location of this relict landscape seems confined to the N-S trending
448 axial part of the peninsula, which is bounded by knickpoints. This questions the
449 scenario of a simple rejuvenation of an antecedent drainage system.
450 Based on a celerity modeling of knickpoint retreat, we show that only upstream
451 Sizhong area can be explained as the result of a wave of regressive erosion through
452 the peninsula (Fig. 8). On the other hand, we have documented numerous capture
453 points arguing for a drainage rearrangement of the drainage system during the last
454 uplift stage (Fig. 10). Thus, the landscape of the Hengchun Peninsula evolves as
455 result of coupling effect of uplift-wave of regressive erosion and drainage captures.
456 We propose to correlate this pattern to the emergence of the southern Taiwan
457 (Suppe, 1981; Pelletier and Stephan, 1986; Liew and Lin, 1987; Ramsey et al., 2007;
458 Stolar et al., 2007). In this case, the drainage rearrangement is no related to a
459 'rejuvenation' of the topography, but rather to a birth of a new landscape. The
460 studied landscape is recent because marine deposits younger than 100 ky are today
461 uplifted in the southern part of the peninsula (Fig. 2). Holocene coral reefs indicate a
462 surface uplift up to 30-40 m for the last 10 ky (Peng et al., 1977; Wang and Burnett,

463 1990) whereas Hengchun limestone suggests a surface uplift around 100-200 m for
464 the last 100 ky (Cheng and Huang, 1975; Chen and Lee, 1990). Assuming the
465 southward propagating model, the ancient coastline and outlet of drainage systems
466 was positioned between the present low-relief of Mutan Ponds and the current
467 coastline. Consequently, before this emergence in Late Pleistocene times, the low
468 relief of Mutan Ponds should be in a direct continuation with the coastline. The
469 landscape during this initial period was likely composed by reduced EW-directed
470 transverse streams, and by the N-S drainage in the Mutan Ponds area at the
471 southern limit of the island (Fig. 12a). The presence of current low reliefs with a N-S
472 trend in the Gutou drainage basin (Fig. 4) argues for such a physiography during
473 this pre-emergence period. The post 100 ky emergence of the submarine
474 morphology resulted in an asymmetrical arrangement of the drainage pattern. The
475 sudden emersion triggers a wave of regressive erosion upstream in drainage basins
476 that were connected to the newly emerged prism. We have documented this wave of
477 regressive erosion in western drainage basins especially for the Sizhong basin. This
478 kind of pattern where transverse drainages coexist with or capture inherited
479 longitudinal paleo-drainages at the termination of tectonic emerging structures has
480 been described in growing folds (e.g. Ramsey et al., 2008).

481 One other possible effect of this emerged asymmetric area to the west is the shift of
482 the drainage divide towards the center of the peninsula, triggering the isolation of
483 the initial low reliefs (Mutan Ponds) (Fig. 12b). Such scenario could explain the
484 current inflection of the drainage divide inside the Hengchun Peninsula.

485 Then, the continuation of regressive erosion of western catchments (Fengkang and
486 Sizhong) will eventually capture these low reliefs. If we consider an endoreic system
487 in Mutan Ponds due to lake deposits in Holocene times up to 2 ky (Lee et al., 2010),
488 the capture event in the upstream part of Fengkang and Sizhong could be only few
489 thousand years old. This can explain why we observe some misfits between eastern
490 and western sub-catchments in Sizhong basin.

491 As the surface uplift propagates southwards, the main drainage divide remained at
492 the eastern flank of the peninsula. The continuous uplift of the low-relief Mutan
493 Ponds increases incision from the east-draining basins. This wave of regressive
494 erosion leads to the second stage of captures. As a result, the eastern basins enlarge
495 their areas due to the west-draining catchments and consequently move the main
496 divide to the west (Fig. 12c, red arrows). Documented captures of the east-draining
497 basins as well as potential points of future piracies substantially support this
498 concept (Fig. 10 and 11). However, the locations of the high and low reliefs as well
499 as the distribution of normalized steepness index k_{sn} suggest the western low-relief
500 terrains to be missing (Fig. 4). It can be related to a submarine topography west to
501 the Hengchun Peninsula where the slopes are too steep to emerge a vast low-relief
502 area or due to fast uplifts of the narrow accretionary wedge generated submarine
503 landslides removing the west flank of the low-relief areas.

504 In summary, the model describing the evolution from the emerging submarine
505 surface to the birth of a new landscape support the transient character of the
506 Hengchun Peninsula. The drainage rearrangement pattern reveals localized waves
507 of knickpoints retreat and shrinkage of the relict landscape as a coherent process

508 (Fig. 13). One of the significant assessments of this study is that the landscapes of
509 the emerging orogens even in the short time span appear to be justified. Our
510 geomorphological analysis and proposed evolutionary model does not allow
511 distinguishing between the different modes of crustal accretion proposed for the
512 Central Range of Taiwan further North: underplating of a subducted crust (Simoes
513 et al., 2007) or ductile flow in the deep crust (Yamato et al., 2009). However, our
514 data and results support a lack of distributed shortening/thrusting across the
515 peninsula, in the southern Central Range. This suggests the region is uplifting as a
516 crustal block, with shortening being accommodated by aseismic deformation in the
517 deeper crust. This might support the onset of crustal shortening below the shallow
518 accretionary wedge as proposed from nearby offshore observations (McIntosh et al.,
519 2013).

520

521 **7. Conclusions**

522 In this study, we focused on the emerging topographic ridge at the southernmost tip
523 of Taiwan orogen, which is the onboard continuity of the offshore accretionary
524 prism. The extraction of geomorphic parameters shows a transient nature of the
525 topography of the Hengchun Peninsula in particular attested by knickpoints
526 distribution and steepness index of rivers. However, we demonstrate that a simple
527 model of regressive erosion following uplift as a rejuvenation of the topography is
528 unlikely at the scale of the entire Peninsula. Knickpoint celerity modeling shows that
529 it is restrained to the upstream part of the Sizhong basin. On the other hand, the
530 current asymmetrical drainage system, linked to a main divide flanked on the

531 eastern side of the Peninsula and where N-S low reliefs (Mutan ponds area) are
532 pinned, is currently affected by numerous capture processes. This indicates a
533 progressive rearrangement of the drainage system confirming the transient nature
534 of the topography. We have proposed an evolutionary model of the Hengchun
535 Peninsula that can explained: (i) how from an antecedent N-S drainage (due to a
536 paleo-northern coastline) it is possible to generate low relief and offset divide (ii)
537 then uplifted and captured by E-W transverse drainages (due to a progressive
538 emergence and shifting coastline). In other words, the Hengchun Peninsula's
539 topography results from a mixing between rejuvenation and drainage
540 reorganization due to the emergence of the southern domain of Taiwan. The scale of
541 this landscape perturbation and the lack of localized tectonic structures argue for an
542 uplifted crustal block origin.

543

544 **Acknowledgments.**

545 This study was supported by National Science Council, Taiwan (NSC 101-2116-M-
546 008-006、NSC 102-2116-M-008 -003、MOST 103-2116-M-008-024).

547

548

549 **Bibliography.**

550

551 Ahnert, F., 1984. Local relief and the height limits of mountain ranges. *American J.*
552 *Science*, 284, 1035-1055.

- 553 Attal, M., Tucker, G.E., Whittaker, A.C., Cowie, P.A., Roberts, G.P., 2008. Modeling
554 fluvial incision and transient landscape evolution: Influence of dynamic channel
555 adjustment. *Journal of Geophysical Research*, 113, F03013.
- 556 Berlin, M.M., Anderson, R.S., 2007. Modeling of knickpoint retreat on the Roan
557 Plateau, western Colorado. *Journal of Geophysical Research- Earth Surface*, 112,
558 F03S06.
- 559 Bishop, P., Hoey, T.B., Jansen, J.D., Artza, I.L., 2005. Knickpoint recession rate and
560 catchment area: the case of uplifted rivers in eastern Scotland. *Earth Surface
561 Processes and Landforms* 30, 767–778.
- 562 Burbank, D.W., 2002. Rates of erosion and their implications for exhumation.
563 *Mineralogical Magazine*, 66, 25–52.
- 564 Chen Y.-G., Liu, T.-K., 1993. Holocene radiocarbon dates in Hengchun Peninsula and
565 their neotectonic implications. *Journal of the Geological Society of China*. 36(4),
566 457-479.
- 567 Chen W.-S., Lee W.-C., 1990. Reconsideration of the stratigraphy of the western
568 Hengchun Hill. *Geology*, 10, 2, 127-140.
- 569 Cheng Y.-M., Huang C.-Y., 1975. Biostratigraphic study in the west Hengchun hill.
570 *Acta Geol. Taiwanica*, 18, 49-59.
- 571 Craddock, W.H., Kirby, E., Harkins, N.W., Zhang, H., Shi, X., Liu, J., 2010. Rapid fluvial
572 incision along the Yellow River during headward basin integration. *Nature
573 Geoscience*, 3(3), 209–213.

574 Crosby, B.T., Whipple, K.X., 2006. Knickpoint initiation and distribution within
575 fluvial networks: 236 waterfalls in the Waipaoa River, North Island, New
576 Zealand. *Geomorphology*, 82, 16-38.

577 Davis, W. M., 1989. The geographical cycle. *Geogr. J.*, 14, 481 – 504.

578 Flint, J.J., 1974. Stream gradient as a function of order, magnitude, and discharge.
579 *Water Resources Research*, 10, 969-973.

580 Fuller, C.W., Willett, S.D., Fisher, D., Lu, C.-Y., 2006. A thermomechanical wedge
581 model of Taiwan constrained by fission-track thermochronometry.
582 *Tectonophysics*, 425, 1-24.

583 Gallen, S.F., Wegmann, K.W., DelWayne R.B., 2013. Miocene rejuvenation of
584 topographic relief in the southern Appalachians. *GSA Today*, 23, 2.

585 Garcia-Castellanos, D., 2006. Long-term evolution of tectonic lakes: Climatic controls
586 on the development of internally drained basins. *Society*, 2398(17), 283–294.

587 Giletycz, S.J., Chang, C.-P., Huang, C.-C., 2012. Geological structure as a crucial factor
588 facilitating the occurrence of typhoon-triggered landslides: Case from Hsiaolin
589 Village, 2009 Typhoon Morakot. *Western Pacific Earth Sciences*, 12, 1, 21-38.

590 Hack, J.T., 1957. Studies on longitudinal stream profiles in Virginia and Maryland.
591 *U.S. Geological Survey Professional Paper*, 294-B, 97.

- 592 Hare, P.H., Gardner T.W., 1985. Geomorphic indicators of vertical neotectonism
593 along the converging plate margins, Nicoya Peninsula, Costa Rica. *Tectonic*
594 *Geomorphology*, 4, 75-104.
- 595 Howard, A., 1994. A detachment-limited model of drainage basin evolution. *Water*
596 *Resources Research*, 30(7), 2261-2285.
- 597 Jackson, J., Norris, R., Youngson J., 1996. The structural evolution of active fault and
598 fold systems in central Otago, New Zealand: evidence revealed by drainage
599 patterns. *Journal of Structural Geology*, 18, 2-3.
- 600 Kirby, E., Whipple, K.X., 2001. Quantifying differential rock-uplift rates via stream
601 profile analysis. *Geology*, 29, 415-418.
- 602 Kirby, E., Whipple, K.X., 2012. Expression of active tectonics in erosional landscapes.
603 *Journal of Structural Geology*, 44, 54-75.
- 604 Lague, D., Davy, P., 2003. Constrains on the long-term colluvial erosion law by
605 analysing slope-area relationship at various tectonic uplift rates in the Siwalik
606 Hills (Nepal). *Journal of Geophysical Research*, 108(B2), 2129.
- 607 Lee, C.-Y., Liew, P.-M., Lee, T.-Q., 2010. Pollen records from southern Taiwan:
608 implications for East Asia summer monsoon variation during the Holocene. *The*
609 *Holocene*, 20, 1, 1-9.

610 Lin, A.-T., Watts, A.B., Hesselbo, S.P., 2003. Cenozoic stratigraphy and subsidence
611 history of the South China Sea margin in the Taiwan region. *Basin Res.*, 15, 453–
612 478.

613 Liew, P.-M., Lin, C.-F., 1987. Holocene tectonic activity of the Hengchun Peninsula as
614 evidenced by the deformation of marine terraces. *Memoir of the Geological*
615 *Society of China*, 9, 241-259.

616 Loget, N., Van Den Driessche, J., 2009. Wave train model for knickpoint migration.
617 *Geomorphology*, 106, 376–382.

618 Loget, N., Davy, P., and Van den Driessche, J., 2006. Mesoscale fluvial erosion
619 parameters deduced from the modeling of the Mediterranean sea-level drop
620 during the Messinian (Late Miocene). *Journal of Geophysical Research*, 111,
621 F03005.

622 Lague, D., Davy P., 2003. Constraints on the long-term colluvial erosion law by
623 analyzing slope-area relationships at various tectonic uplift rates in the
624 Siwaliks Hills (Nepal). *Journal of Geophysical Research*, 108 (B2), 2129.

625 McIntosh, K.D., Kuochen, H., Van Avendonk, H.J., Lavier, L.L., Wu, F.T., Okaya, D.A.,
626 2013. Two-dimensional seismic velocity models of southern Taiwan from
627 TAIGER transects. *American Geophysical Union, Fall Meeting*, T21G-05.

628 Mesalles, L., Mouthereau, F., Bernet, M., Chang, C-P., Lin, T-S., Fillon, C., Sengelen, X.,
629 2014. From submarine continental accretion to arc-continent orogenic

630 evolution: the thermal record in the Taiwan mountain belt. *Geology*. doi:
631 doi:10.1130/G35854.1

632 Pelletier, B., Stephan, J.F., 1986. Middle Miocene obduction and late Miocene
633 beginning of collision registered in the Hengchun Peninsula: Geodynamics
634 implications for the evolution of Taiwan. *Memoir of the Geological Society of*
635 *China*, 7, 301-324.

636 Peng, T.-H., Li, Y.-H., Wu, F.-T., 1977. Tectonic uplift rates of the Taiwan island since
637 the Early Holocene. *Memoir of the Geological Society of China*, 2, 57-69.

638 Ramsey, L.A., 2006. Topographic evolution of emerging mountain belts. PhD Thesis,
639 *not published*.

640 Ramsey, L.A., Walker, R.T., Jackson J., 2007. Geomorphic constraints on the active
641 tectonics of the southern Taiwan. *Geophysics*, 170, 1357-1372.

642 Ramsey, L.A., Walker, R.T., and Jackson, J., 2008. Fold evolution and drainage
643 development in the Zagros mountains of Fars province, SE Iran. *Basin Research*,
644 20, 23-48.

645 Roberts, G., White, N. J., 2010. Estimating Uplift Rate Histories from River Profiles
646 using African Examples. *Journal of Geophysical Research- Solid Earth*, 115.
647 B02406. ISSN 0148-0227

648 Rosenbloom, N.A., Anderson, R.S., 1994. Hillslope and channel evolution in a marine

649 terraced landscape, Santa Cruz, California. *Journal of Geophysical Research*, 99 (B7),
650 14013–14029.

651 Siame, L.L., Angelier, J., Chen, R.-F., Godard, V., Derrieux, F., Bourlès, D.L., Braucher,
652 R., 2011. Erosion rates in an active orogen (NE-Taiwan): A confrontation of
653 cosmogenic measurements with river suspended loads. *Quaternary*
654 *Geochronology*, 6(2), 246–260.

655 Simoes, M., Avouac, J.P., Beyssac, O., Goffe, B., Farley, K.A., Chen, Y.-G., 2007.
656 Mountain building in Taiwan: a thermokinematic model. *J. Geophys. Res.*, 112,
657 B11405.

658 Simoes M., Beyssac, O., Chen, Y.-G., 2012. Late Cenozoic metamorphism and
659 mountain building in Taiwan: A review. *Journal of Asian Earth Sciences*, 46, 92-
660 119.

661 Snyder N.P., Whipple, K.X., Tucker, G.E., Merritts, D.J., 2000. Landscape response to
662 tectonic forcing: Digital elevation model analysis of stream profiles in the
663 Mendocino triple junction region, northern California. *GSA Bulletin*, 112, 1250-
664 1263.

665 Stolar, D.B., Willet S.D., Montgomery D.R., 2007. Characterization of topographic
666 steady state in Taiwan. *Earth and Planetary Science Letters*, 261, 421-431.

667 Suppe, J., 1981. Mechanics of mountain building and metamorphism in Taiwan.
668 *Mem. Geol. Soc. China*, 4, 67-89.

669 Walker, R.T., Ramsey, L.A., Jackson, J., 2011. Geomorphic evidence for ancestral
670 drainage patterns in the Zagros Simple Folded Zone and growth of the Iranian
671 plateau. *Geological Magazine*, 148, 901–910.

672 Wang, C.-H., Burnett, W.C., 1990. Holocene mean uplift rates across an active plate-
673 collision boundary in Taiwan. *Science*, 248, 4952, 204-206.

674 Whipple, K.X., Tucker, G.E., 1999. Dynamics of the stream-power river incision
675 model: implications for height limits of mountain ranges, landscape response
676 timescales, and research needs. *Journal of Geophysical Research*, 104(B8),
677 17661-117674.

678 Whipple, K.X., 2001. Fluvial landscape response time: how plausible is steady-state
679 denudation? *American Journal of Science*, 301, 313-325.

680 Whipple, K.X., 2004. Bedrock Rivers and the Geomorphology of Active Orogens.
681 *Annual Review of Earth and Planetary Sciences*, 32(1), 151–185.

682 Whipple K.X., Wobus, C.W., Kirby, K., Crosby, B., Sheehan, D., 2007. New Tools for
683 Quantitative Geomorphology: Extraction and Interpretation of Stream Profiles
684 from Digital Topographic Data. *Geological Society of America Annual Meeting*
685 *Course Notes*.

686 Whipple K.X., DiBiase R.A., Crosby B.T., 2013. Bedrock rivers. *Treatise on*
687 *Geomorphology*. 9, 550-573.

688 Whittaker, A.C., Cowie, P.A., Attal, M., Tucker, G.E., Roberts, G.P., 2007. Bedrock
689 channel adjustment to tectonic forcing: Implications for predicting river
690 incision rates. *Geology*, 35(2), 103.

691 Willett, S.D., Brandon, M.T., 2002. On steady states in mountain belts. *Geology*, 30(2),
692 175.

693 Willett, S.D., Fisher, D., Fuller, C., En-Chao, Y., Chia-Yu, L., 2003. Erosion rates and
694 orogenic-wedge kinematics in Taiwan inferred from fission-track
695 thermochronometry. *Geology*, 31(11), 945.

696 Wobus, C.W., Crosby B.T., Whipple, K.X., 2006. Hanging valleys in fluvial systems:
697 Controls on occurrence and implications for landscape evolution. *Journal of*
698 *Geophysical Research*, 111, F02017.

699 Yamato, P., Mouthereau, F., Burov, E., 2009. Taiwan mountain building: insights from
700 2-D thermomechanical modelling of a rheologically stratified lithosphere,
701 *Geophysical Journal International*, 176(1), 307–326.

702 Yang, T.-N., Lee, T.-Q., Meyers, P.A., Song, S.-R., Kao, S.-J., Löwemark, L., Chen, R.-F.,
703 2011. Variations in monsoonal rainfall over the last 21 kyr inferred from
704 sedimentary organic matter in Tung-Yuan Pond, southern Taiwan. *Quaternary*
705 *Science Reviews*, 30(23-24), 3413–3422.

706

707

708

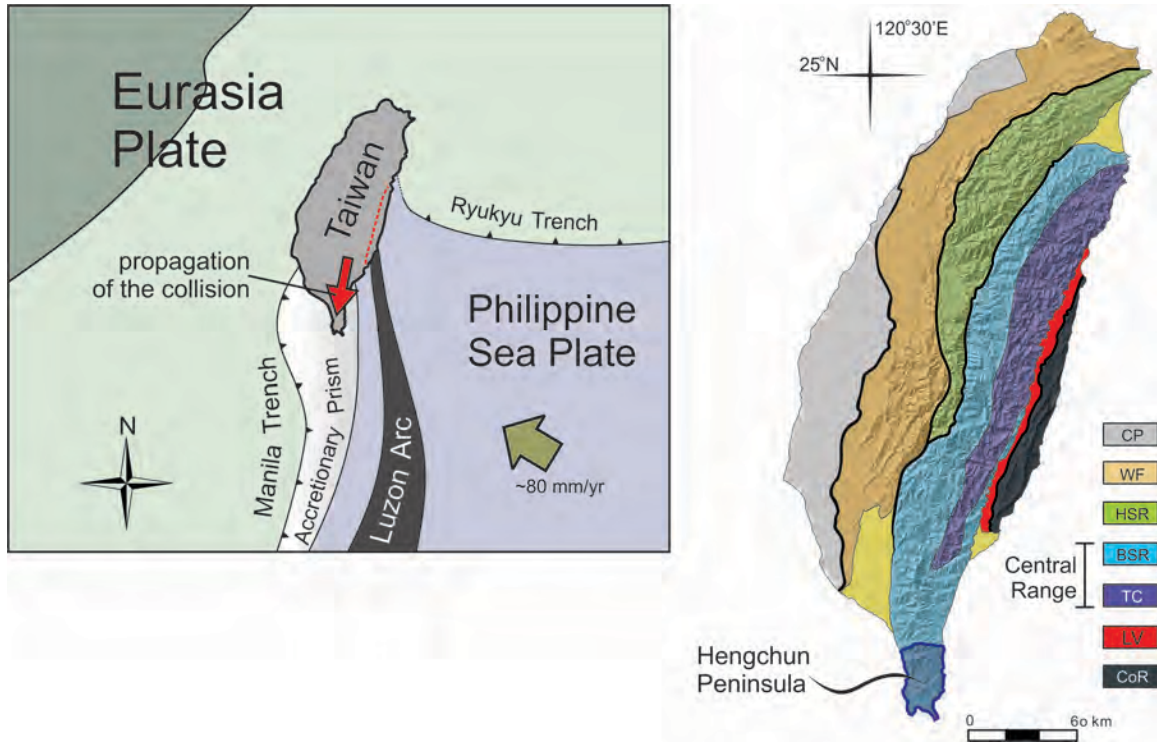


Fig. 1. Geological setting of Taiwan arc-continent collision. Left: map showing the oblique collision between Eurasia and Philippine Sea plates resulting in the progressive emergence of Taiwan orogen towards the south (red arrow). Right: geological provinces of Taiwan: CP- Coastal Plain; WF- Western Foothills; HSR- Hsuehshan Range; BSR- Backbone Slate Range; TC -Tananao Complex; LV- Longitudinal Valley; CoR- Coastal Range.

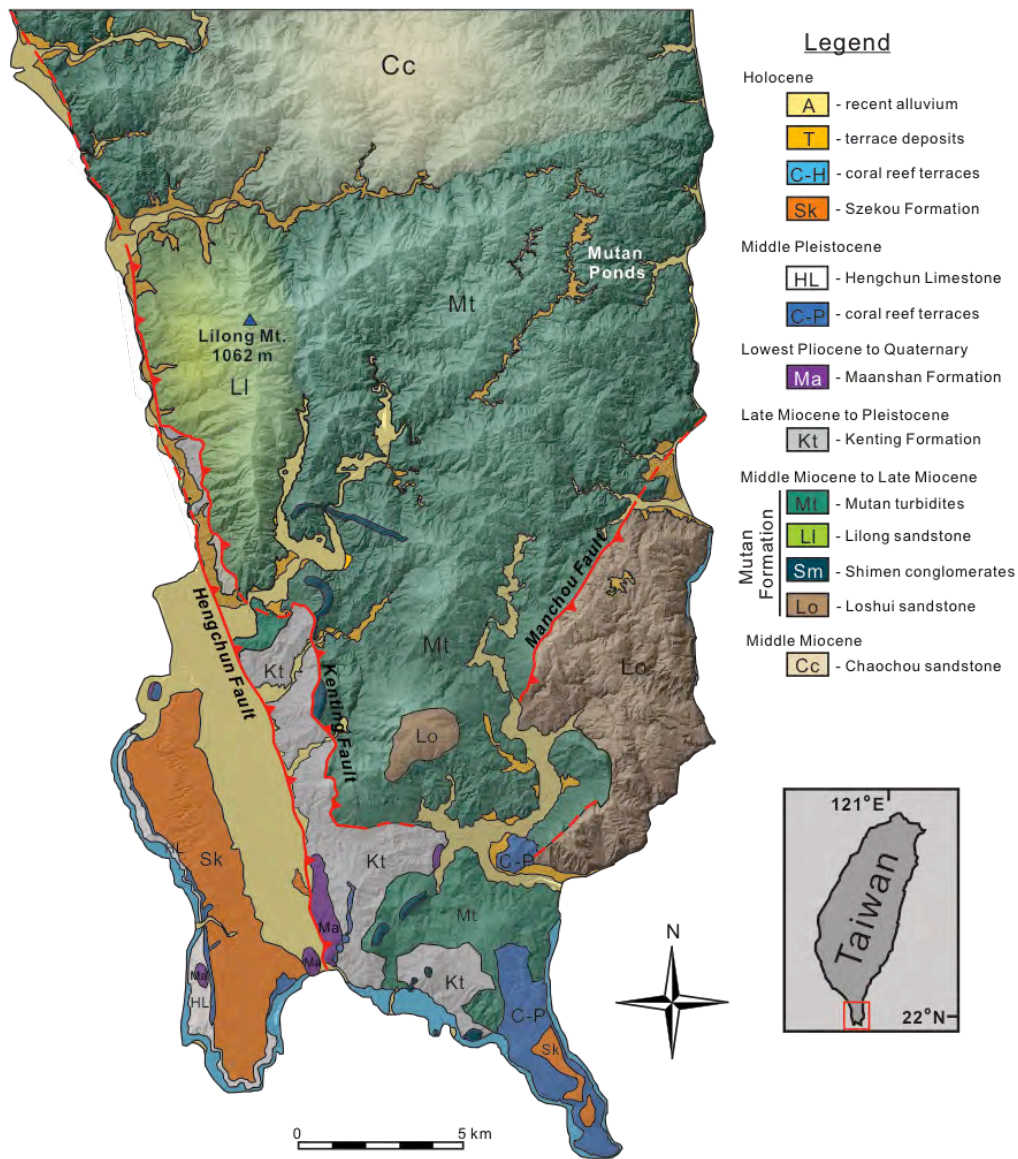


Fig. 2. Geological map of the Hengchun Peninsula (modified after CGS 1989; Chang et al., 2002; Yen, 2003; Chen et al., 2005 and others)

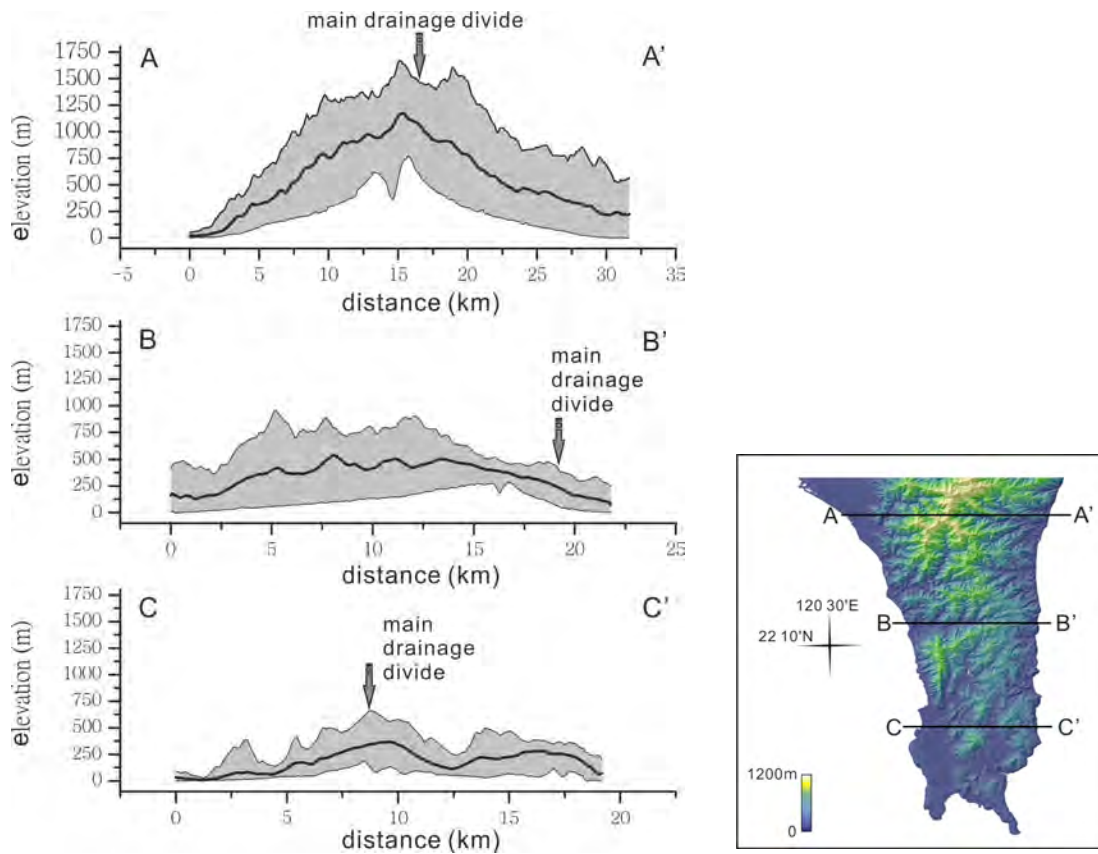


Fig. 3. Swath topography profiles (with 10 km window) across the southern Central Range, northern and central Hengchun Peninsula, respectively. Each profile shows focal statistics of the highest, mean and the lowest elevation, respectively. The arrows locate the boundary of the main divide. The profile B-B' shows an offset of the main divide and the highest topography point- Lilong Mt.

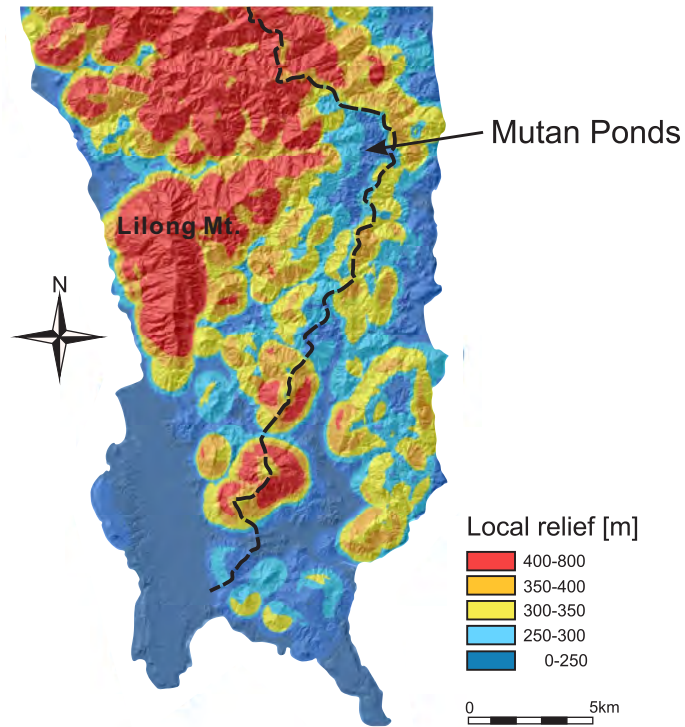


Fig. 4. Relief map of the Hengchun Peninsula (computed with 5 km sliding window). N-S elongated low relief stretch at the eastern part of the peninsula from Mutan Ponds southwards (blue area). Note the main drainage divide (black-dashed line) cutting across the low relief N-S trending area.

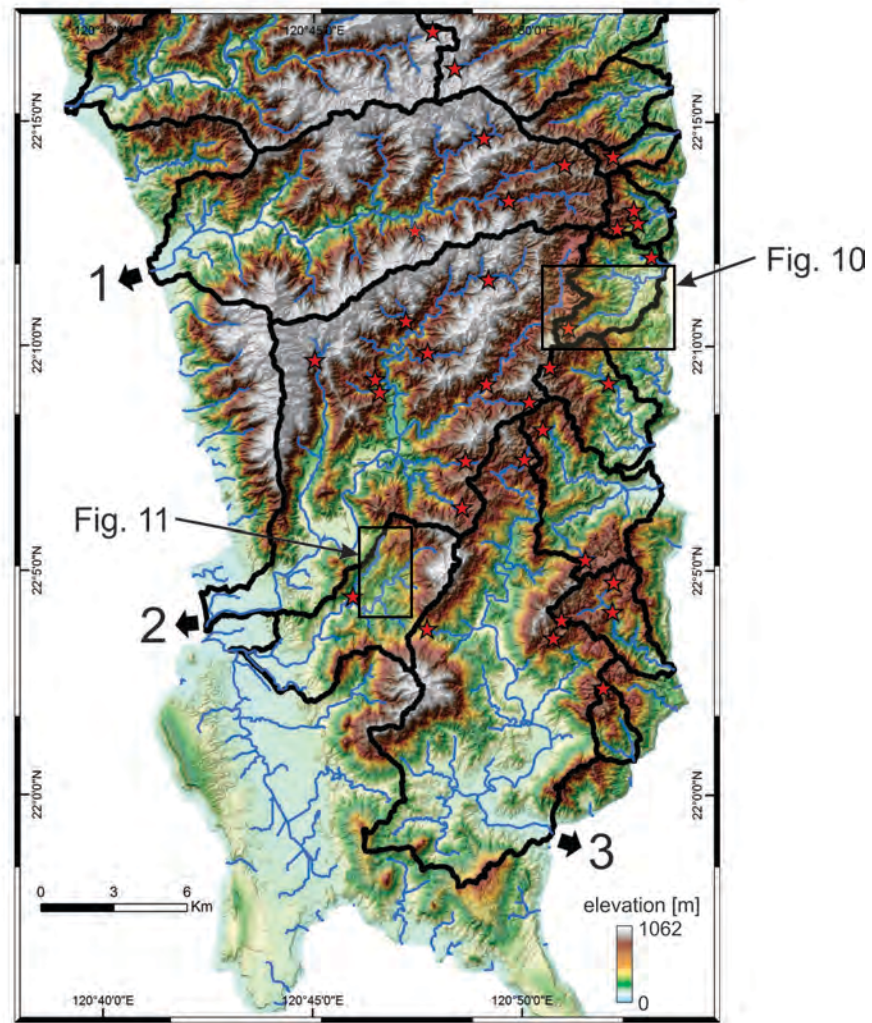


Fig. 5. Drainage basins of the Hengchun Peninsula: 1- Fengkang, 2- Sizhong, 3- Gutou basins. Red stars represent main knickpoints.

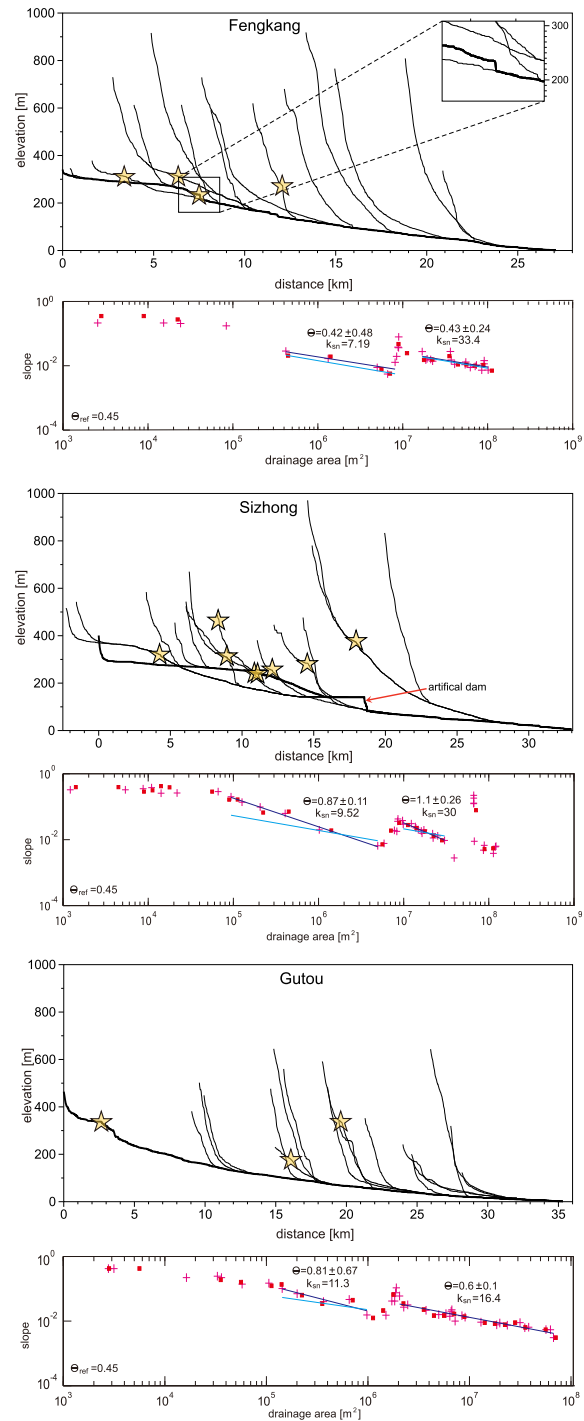


Fig. 6. Long and log/log slope-area profiles of the major basins of the Hengchun Peninsula: Fengkang, Sizhong and Gutou.

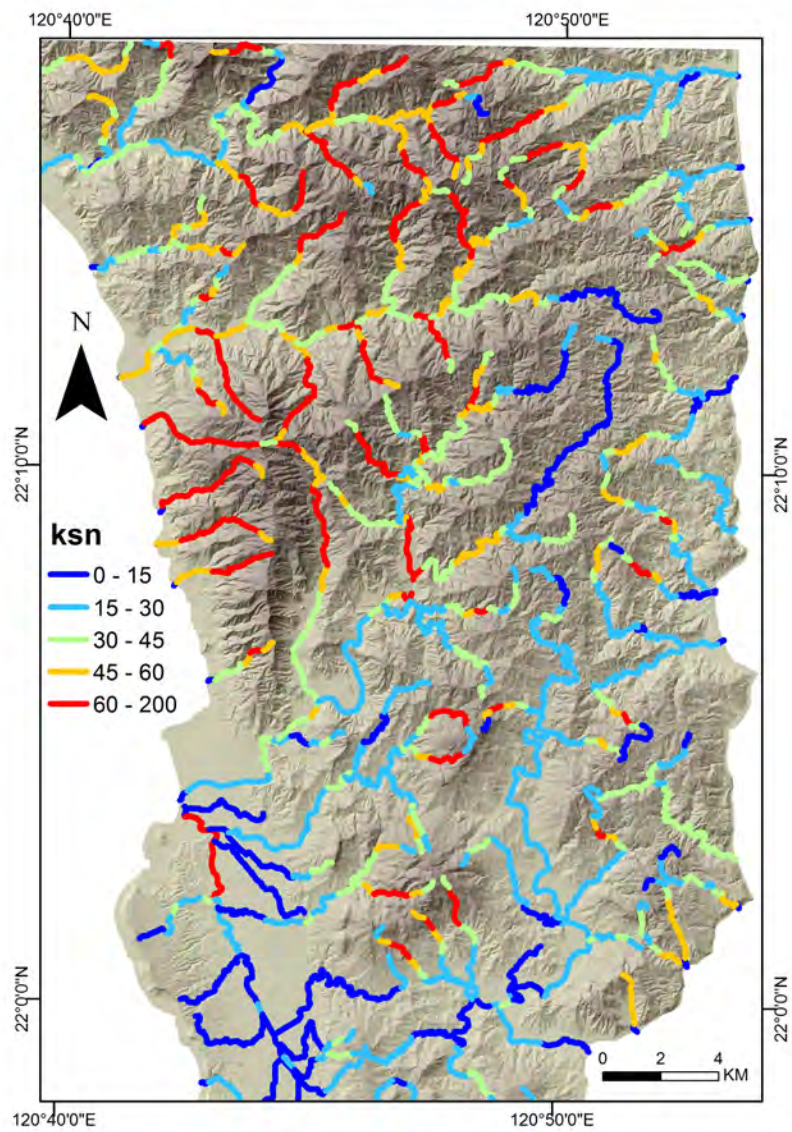


Fig. 7. Normalized steepness index (ksn) of the channels at Hengchun Peninsula 9 (concavity index θ_{ref} for all channels is 0.45)

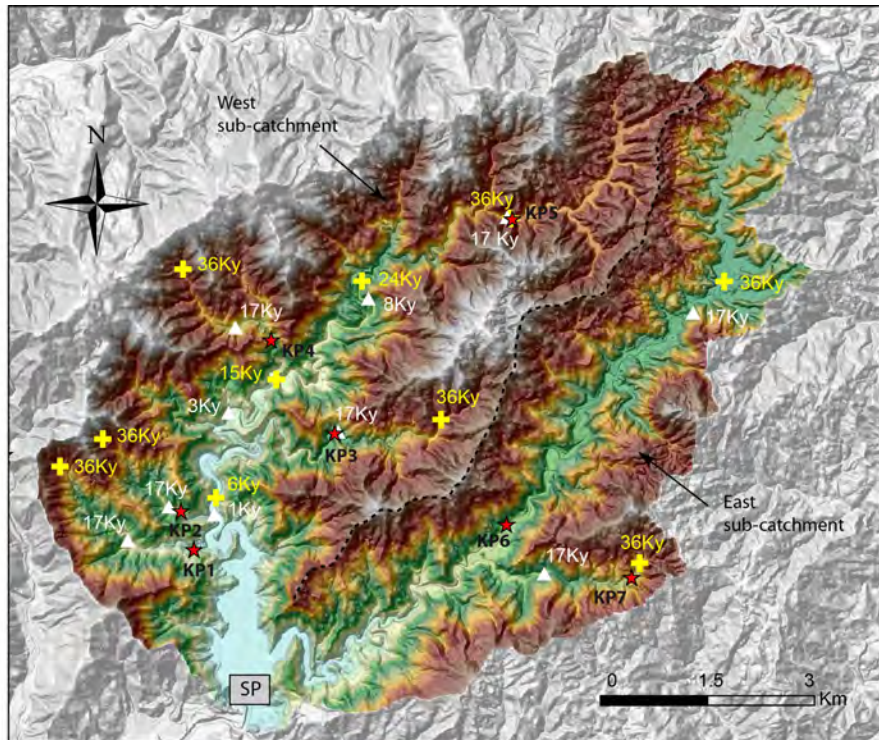


Fig. 8. Celerity modeling of the knickpoints migration in the Sizhong basin (location in Fig. 5 and 13) with two end-members. Red star shows observed knickpoints. White cross represents a modeling of the migration with a celerity modeling where $dx/dt=0.0001A^{0.5}$ (Loget and Van Den Driessche, 2009). Blue triangle represents the modeling with $dx/dt=0.0000079A^{1.1125}$ (Crosby and Whipple, 2006). Time stopped for all points at $T=12$ ky and $T=17$ ky, respectively. SP- represents the starting point.



Fig. 9. Photograph looking to the west showing active regressive erosion in the upstream part of a tributary of the Xuhai basin (see location in figure 10).

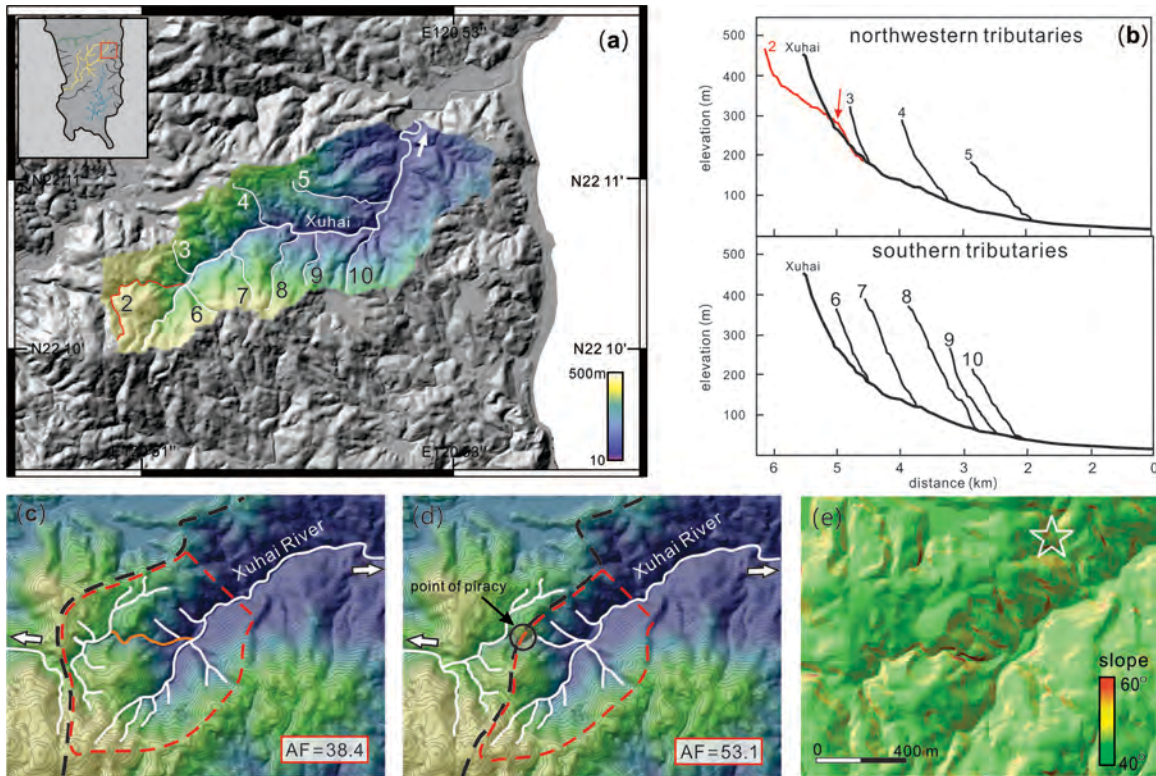


Fig. 10. Capture processes in the western part of the Xuhai basin. a) DEM with drainage of the southern part of the the Xuhai basin showing recent capture channel in orange (location in Fig. 5). (b) Knickpoint of the upper channel (red arrow) indicates the capture point (a). (c) Present setting of the Xuhai upstream. Note the flow direction of the western tributaries and curve of the main drainage divide (black dashed line). (d) Potential scenario before the capture. The Asymmetry Factor (AF) shows almost symmetrical pattern of the Xuhai upstreams. (e) High slope values of the Xuhai channel suggest dynamic incision processes what also fueled the erosion leading to the capture. White star shows the location of the tributary presented in figure 9.

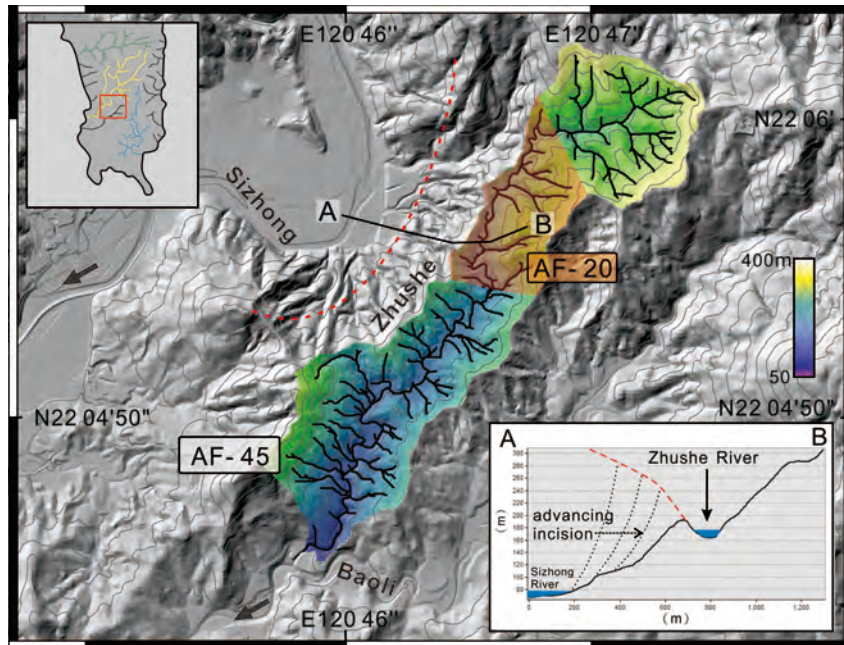


Fig. 11. Capture processes of the Zhushe River (tributary of the Baoli River) by the Sizhong River (location in Fig. 5). Due to progressive erosion of the lower elevated meander of the Sizhong River, the western tributaries of the central-upper part of the Zhushe sub-basin are missing. Note very low Asymmetry Factor (AF) of the marked area (orange) *versus* whole Zhushe sub-basin. A potential capture become apparent at the marked area in orange.

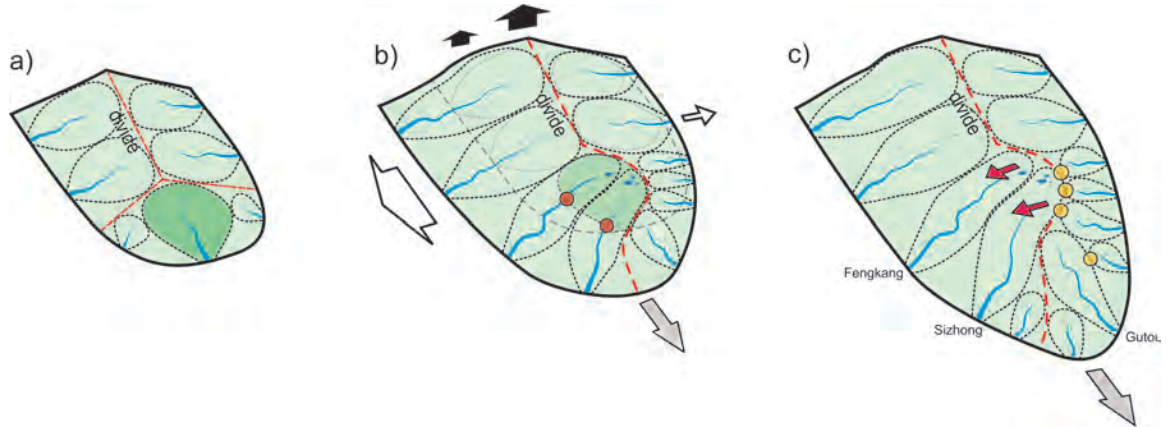


Fig. 12. Evolutionary model of the Hengchun Peninsula. (a) Tip of an emerging orogen develops channels in fan-shape pattern, where N-S drainage is the future Mutan Ponds area. (b) Asymmetric emergence elongates the channels and triggers the isolation of the initial low reliefs- Mutan Ponds. (c) The continuous uplift of the low-relief Mutan Ponds increases incision from the east-draining basins leading to the second stage of captures moving the main divide to the center of the peninsula.

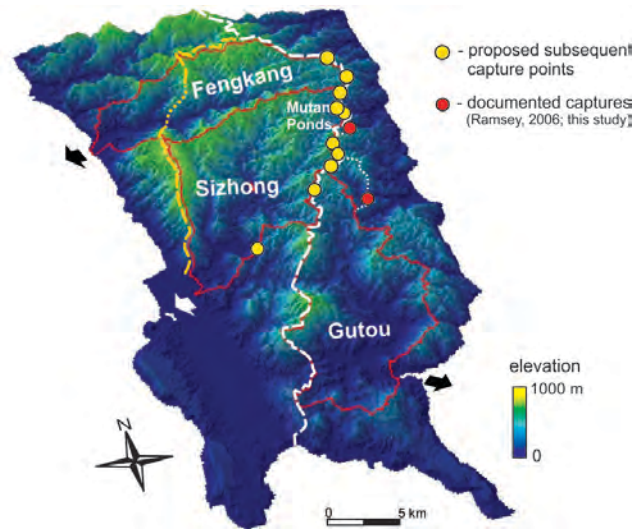


Fig. 13. 3-D view of the Hengchun Peninsula's topography and its main basins. White dashed line shows the main divide, a yellow line shows highest topography ridge. A dotted yellow line shows the break of the highest topography ridge.